Performance analysis of different organic Rankine cycle configurations on board liquefied natural gas-fuelled vessels

Baldasso, Enrico; Andreasen, Jesper Graa; Meroni, Andrea; Haglind, Fredrik

Published in:
Proceedings of ECOS 2017: 30th International Conference on Efficiency, Cost, Optimization, Simulation and Environmental Impact of Energy Systems

Publication date:
2017

Document Version
Peer reviewed version

Performance analysis of different organic Rankine cycle configurations on board liquefied natural gas-fuelled vessels

E. Baldasso[a], J. G. Andreasen[b], A. Meroni[c], and F. Haglind[d]

[a]Technical University of Denmark, Kgs. Lyngby, Denmark, enbald@mek.dtu.dk
[b]Technical University of Denmark, Kgs. Lyngby, Denmark, jgan@mek.dtu.dk
[c]Technical University of Denmark, Kgs. Lyngby, Denmark, andmer@mek.dtu.dk
[d]Technical University of Denmark, Kgs. Lyngby, Denmark, frh@mek.dtu.dk

Abstract:

Gas-fuelled shipping is expected to increase significantly in the coming years. Similarly, much effort is devoted to the study of waste heat recovery systems to be implemented on board ships. In this context, the organic Rankine cycle (ORC) technology is considered one of the most promising solutions. The ORC favorably compares to the steam Rankine cycle because of its simple layout and high efficiency, achievable by selecting a working fluid with desirable properties. This paper aims at assessing the fuel savings attainable by implementing ORC units on board vessels powered by liquefied natural gas (LNG). The study compares the performance of six different ORC configurations both in design and off-design operation, and provides guidelines with respect to the most promising heat sources and sinks to be utilized by an ORC unit in order to maximize the annual fuel savings. In addition, this paper describes a novel ORC layout rejecting heat to two heat sinks. The results indicate equivalent fuel savings up to 8.9 % when harvesting heat from the exhaust gases, and that the novel configuration ensures an increment of the ORC design power output up to 41 % when utilizing the jacket cooling water as heat source.

Keywords:

Organic Rankine cycles, waste heat recovery, liquefied natural gas, part-load, fuel savings

1. Introduction

Most of the vessels in the world are currently powered by diesel engines fueled by Heavy Fuel Oil (HFO). HFOs are cheap fuels, but they contain high levels of asphalt, carbon residues, sulfur and metallic compounds [1]. The International Maritime Organization (IMO) recently introduced an updated legislation framework setting constraints for emissions of greenhouse gases, NO_x and SO_x [2 - 6]. In order to comply with the new regulation, a number of possible solutions have been investigated, including the development of new propulsion systems [7]. Nonetheless, the introduction of techniques such as the Selective Catalytic Reduction (SCR) and the Exhaust Gas Recirculation (EGR) might be required in order to fulfil the NO_x emission constraints [8 - 9]. In this context, the possibility of utilizing Liquefied Natural Gas (LNG) as a marine fuel is gaining increasing interest. The use of LNG as a shipping fuel is not a novel idea, since LNG carries have been running on LNG for more than 40 years [10]. In addition, the proved reliability of the dual fuel marine engines [11] and the environmental benefits of using LNG as a fuel [12] are pushing toward a wider adoption of this solution in the shipping industry. Concurrently, increasing attention is devoted to the study of waste heat recovery (WHR) units that can convert the waste heat available on board into power, leading to lower fuel consumptions and emissions of pollutants. The use of Steam Rankine cycles (SRC) as a WHR unit on board vessels is a well-established solution, leading to fuel savings up to 10 % [13]. An alternative to the SRC is the use of an organic Rankine cycle (ORC) unit. The ORC operates similarly to an SRC, but the working fluid is an organic compound that enables the attainment of a good thermal match between the cycle and the heat source. At present, only a few ORC units on board vessels running on heavy fuel oil exist worldwide [14 - 15]. Larsen et al. [16] compared the implementation of traditional SRC, ORC and Kalina cycles on

board large ships and reported that the ORC was the most promising technology, leading to an increment by 7 % of the onboard power production. Andreasen et al. [17] investigated the off-design performance of a traditional dual SRC and of an ORC unit and concluded that the ORC process enabled higher performance at low engine loads due to a limited use of turbine throttling compared to the SRC process. When designing a WHR unit for the utilization of the main engine exhaust gases, particular care has to be taken in order to avoid corrosion problems due to the possible formation of sulfuric acid in the WHR boiler. MAN Diesel & Turbo [18] suggested that the dew point temperature for sulfur condensation is around 135 °C, when utilizing a fuel with an average sulfur content of 2.9 %. The risk for sulfur corrosion is reduced in LNG-fuelled vessels, as sulfur is present only in the pilot fuel oil.

The LNG fuel is stored on board in liquid state at – 162 °C [19] and a preheating process is necessary prior to the injection of the fuel in the engine. The exploitation of the LNG cold energy has been already investigated in the past, but most of the studies focused on the utilization of the cryogenic energy in LNG regasification terminals [20]. Regarding on board implementations, Sung et al. [21] studied a dual loop ORC unit tailored for dual fuel engines. The upper ORC loop recovered heat from the exhaust gases, while the bottom loop harvested energy from the jacket cooling water and the LNG preheater. The results suggested that the high temperature cycle contributed to 82.3 % of the power production and that the thermal efficiency of the low temperature loop could be as high as 22.7 %. Soffiato et al. [22] investigated the use of low temperature ORC systems on board LNG carriers and concluded that two-stage ORC configurations, due the higher complexity, could reach higher net power outputs compared to single-stage configurations. Senary et al. [23] analyzed the implementation of a single loop SRC on board a LNG carrier and estimated a possible reduction of the CO_2 and NO_x emissions by 16.9 % and 36.3 % respectively. The review of the state-of-the-art presented above highlights that the implementation of ORC units on board vessels represents a viable solution to decrease the emission of pollutants and the fuel consumption. Nevertheless, the majority of the existing works focuses on HFO-fuelled vessels, while there is a lack of studies investigating the achievable fuel saving on board LNG-fuelled vessels. In addition, there is a lack of studies investigating the part load performance of cryogenic ORC units exploiting the LNG cold energy on board vessels.

The objective of this paper is to assess the fuel savings achievable by implementing an ORC unit on board an LNG-fuelled vessel. The performance of cryogenic ORC units exploiting the LNG cold energy on board vessels is investigated both at design and off-design conditions, enabling the estimation of the unit performance at different load points. A novel double-condenser ORC configuration rejecting heat both to the seawater and the LNG preheating is presented, optimized and discussed. The work is innovative in the sense that previous works were limited to design point investigations and thus it was not possible to estimate the achievable annual fuel savings. In addition, the novel double-condenser ORC configuration differs from the previously investigated solutions as it suggests the utilization of the LNG low temperature heat as a way to boost the performance of the traditional ORC cycle, rather than in a stand-alone cycle.

The paper is structured as follows: Section 2 explains the applied methods. Section 3 presents and discusses the results. Finally, the conclusions are outlined in Section 4.

2. Methods

This study investigated the implementation of WHR units on board a hypothetical vessel equipped with a 7G95ME-C9.5 GI MAN Diesel & Turbo dual fuel two-stroke marine engine with low pressure SCR tuning. The choice of an engine with low pressure SCR tuning ensured higher temperatures of the exhaust gases and thus an increased power production from the ORC unit. The low pressure SCR tuning was simply used to simulate a WHR tuning, meaning that a SCR system

was not considered as part of the machinery system. The CEAS engine calculation tool [24] from MAN Diesel & Turbo was utilized to retrieve the engine data. Table 1 shows information regarding the engine operation and the availability of the considered energy streams. SPOC denotes the specific pilot oil consumption, while SGC is the specific gas consumption. The LNG fuel mass flow rate was derived from the engine SGC, while the jacket water (JW) mass flow rate was calculated from the provided volumetric flow rate. The engine is supplied with gas at 250 – 300 bar depending on the load [25]. The JW heat is not fully available for the ORC unit, as 400 kW are assumed to be utilized by the onboard fresh water generators, at all engine loads. The need for HFO preheating is strongly reduced for ships powered by dual fuel engines, but still there is a need for some service steam for heating purposes. However, these requirements were not considered, as this study focused on the comparison between different ORC configurations.

Table 1. Main engine performance and waste heat sources at different engine loads

Load [%]	Power [kW]	SPOC [g/kWh]	SGC [g/kWh]	$\dot{m}_{ex}$ [kg/s]	T_{ex} [°C]	JW heat [kW]	T_{jw} [°C]	$\dot{m}_{jw}$ [kg/s]	$\dot{m}_{LNG}$ [kg/s]
100	36,820	5.8	135.8	79.1	261	4,380	85	69.47	1.39
75	27,615	7	129.7	60.9	253	3,570	85	69.47	0.99
50	18,410	9.2	127.1	42.6	268	2,760	85	69.47	0.65
25	9,205	14.6	129	22.4	285	1,940	85	69.47	0.33

The study assumed that the vessel operates with full boil-off gas re-liquefaction and that the gas was supplied to the engine with a high-pressure pump and a gas vaporizer. Six different ORC configurations, subdivided into two cases, were considered for on board implementation. The first three configurations (case A) utilized the main engine exhaust gases and the jacket cooling water as heat sources, while the last three configurations (case B) harvested heat only from the jacket cooling water. Regarding the heat sinks, the following possibilities were investigated: 1) seawater, 2) seawater and LNG preheating, and, 3) LNG preheating. Configurations of case A feature also an internal recuperator, which enables to increase the boiler feed temperature and thus to limit the sulfuric acid formation in the WHR boiler [18]. The boiler feed temperature lower limit was set to 110 ° C for this study. The influence of this assumption on the results is discussed in Section 3. Figure 1 shows a sketch of the various configurations.

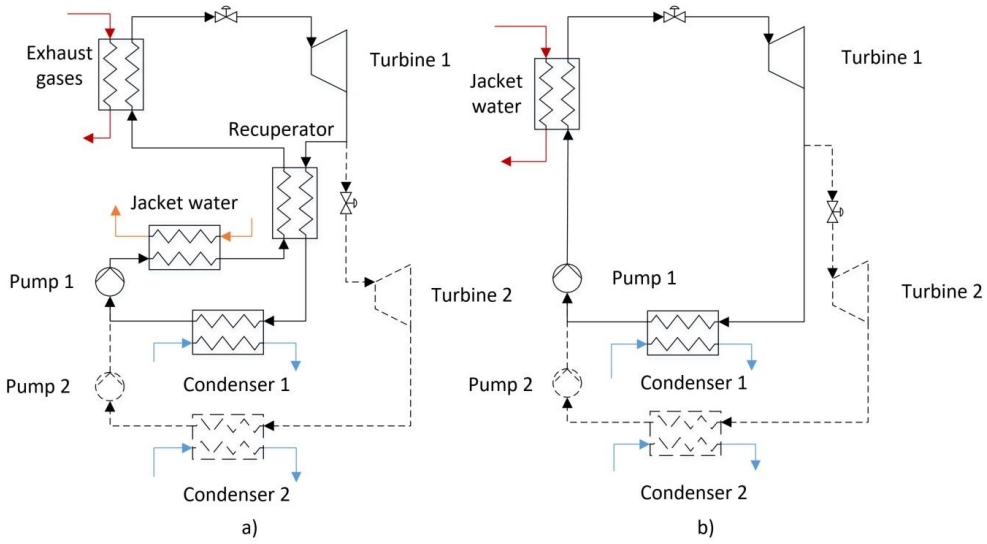

Fig. 1. Sketch of the considered ORC configurations: a) cases A; b) cases B; The dotted lines represent the additional components included for cases A2 and B2.

In configurations A2 and B2, a fraction of the working fluid mass flow rate was supplied to the second expander instead of going through the seawater condenser. The second expander ensured the production of higher net power outputs compared to the cases featuring only the seawater condenser (A1 and B1) and enabled the exploitation of the energy released by the LNG during the preheating process. The cases A3 and B3 were investigated since they have the potential for high efficiency.

One of the most important factors in the performance of ORC systems is the selection of a suitable working fluid. A wide range of working fluids have investigated in literature for moderate [26 - 29], low [22 - 23, 26, 28 - 30], and cryogenic temperature [20, 31 - 32] ORC systems. The possible working fluid candidates were limited to commercially available fluids [33 - 35] not affected by thermal stability issues in the considered temperature range [36]. In addition, R1233zd(E) and R1234yf were investigated for the case B configurations, since they were proposed as replacement fluids for R134a and R245fa [37]. Table 2 shows the list of the selected fluids for the various configurations. Flammability and toxicity indexes are provided according to the standard NFPA 704, critical temperatures and melting points were retrieved from Coolprop [38].

Table 2. List of the selected working fluids

Fluid	Configuration	Tc [K]	GWP	ODP	Thermal stability [K]	Melting point [K]	Flamm/ Tox
cyclopentane	all	511.72	< 25	0	513 - 548	179.26	3/1
isobutane	all	407.84	20	0	n.a.	134.85	4/0
ipentane	all	460.35	43	1	500 - 588	113.26	4/1
butane	all	425.12	4	0	563 - 693	134.76	4/1
n-pentane	all	469.7	42	0	573 - 588	143.15	4/1
MM	A1	518.75	n.a.	n.a.	573	214	4/1
toluene	A1	591.75	n.a.	n.a.	> 588	178.15	3/2
R134a	B1-2-3	374.25	1300	0	n.a.	176.48	0/1
R245fa	all	427.16	1030	0	523 - 573	166.48	2/0
R1233zd(E)	B1-2-3	435.75	1	0	n.a.	166.15	0/2
R1234yf	B1-2-3	367.85	4	0	n.a.	123.15	4/1

When optimizing the various ORC configurations, the maximum and minimum allowable pressures were set to 30 bar and 4.5 kPa respectively, following the indications by Rayegan et al. [39], Drescher and Brüggeman [40], and MAN Diesel & Turbo [41]. Moreover, the work was limited to subcritical cycle configurations, with a maximum limit of 0.8 in reduced pressure, in order to avoid problems during operation near the critical point. The freezing temperature at the condenser pressure was estimated by assuming that the melting line of the various fluids can be approximated with a straight line connecting the triple point to the melting point, provided at 1 bar. In order to avoid having very high viscosities at the inlet of pump 2, a minimum operational limit of 10 degrees above the estimated freezing point was considered. The ORC cycle performance was calculated by means of an updated version of the ORC model previously validated in Andreasen et al. [42] (maximum relative deviation of 3.27 % compared to other studies in literature). The ORC unit was designed for main engine load of 75 % and the ORC net power output was set as the objective function in the optimization procedure. The cycle net power output was calculated as follows:

$$\dot{W}_{Net} = \left(\dot{W}_{t1} + \dot{W}_{t2}\right)\eta_{gear}\,\eta_{gen} - \dot{W}_{p1} - \dot{W}_{p2} - \dot{W}_{p,sw}, \quad (1)$$

Where $\dot{W}_{p,sw}$, $\dot{W}_{p,1}$, $\dot{W}_{p,2}$, $\dot{W}_{t,1}$ and $\dot{W}_{t,2}$ represent the power absorption of the seawater pump and ORC pumps and the power production of the ORC turbines, respectively. While η_{gear} and η_{gen} represent the efficiencies of the gearbox and of the electrical generator. The decision variables of the optimization process were the turbine inlet pressure, the superheating degree at the turbine inlet, the

working fluid condensation temperature in the LNG condenser (configurations A2, A3, B2, B3) and the fraction of mass flow supplied to the LNG condenser (configurations A2 and B2). The pressure losses in the heat exchangers were neglected. The expanders and the pumps were modelled with fixed values of the isentropic efficiency. Table 3 lists the parameters that were fixed in the optimization procedure.

Table 3. List of the fixed parameters in the ORC optimization

Parameter	Case A	Case B	Unit
Heat source			
Main heat source	Exhaust gases	Jacket water	-
Main heat source temperature	253	85	°C
Mass flow	60.9	69.47	kg/s
Secondary heat source	Jacket water	-	
Secondary heat source temperature	85	-	°C
Mass flow rate	69.47	-	kg/s
Heat exchangers			
Minimum boiler superheating	5	5	°C
Minimum boiler feed temperature	110	-	°C
JW preheater outlet temperature	80	-	°C
Boiler pinch point temperature $\Delta T_{pp,boil}$	20	5	°C
LNG condenser pinch point temperature $\Delta T_{pp,LNG}$	10	10	°C
Recuperator pinch point temperature $\Delta T_{pp,rec}$	10	-	°C
Sea water condenser			
Condensation temperature	30	30	°C
Sea water inlet temperature	15	15	°C
Sea water temperature increase	5	5	°C
Sea water pump head	2	2	bar
Sea water pump efficiency	0.7	0.7	-
LNG condenser			
LNG inlet temperature	-165	-165	°C
LNG pressure	300	300	bar
LNG mass flow	1	1	kg/s
Expander, pump and generator			
Turbine isentropic efficiency $\eta_{is,t}$	0.85	0.85	-
Pump isentropic efficiency $\eta_{is,p}$	0.7	0.7	-
Electric generator efficiency η_{gen}	0.98	0.98	-
Gearbox efficiency η_{gear}	0.98	0.98	-

This work included also the development of part-load models of the thermodynamic cycle. The purpose of these models is to investigate the behavior of the different ORC configurations when the main engine load decreases. The input parameters of the part-load models were the main engine load, defined by the power and temperature of the waste heat sources, and the ORC design parameters, represented by the design efficiency of the various components and the UA values of the heat exchangers. The part-load performance was estimated for the main engine load ranging from 75 to 25 %, since no data were available about the engine operation at lower loads. The variation of the turbine isentropic efficiency was estimated using the relationship presented by Schobeiri [43], while the relationship between the mass flow rate and the pressures was assumed to be governed by the Stodola equation [44]. These correlations were originally derived for multistage axial steam turbines, but were previously utilized to estimate the behavior of ORC turbines in

geothermal power plants [45], solar systems [46] and WHR applications from both diesel engines [47] and gas turbines [48]. The performance of the electric generator was derived from the procedure presented by Haglind and Elmegaard [49], while the pump part-load efficiency was obtained from a technical datasheet of Grundfos [50]. The seawater pump efficiency was assumed constant. The boiler (subdivided into pre-heater, evaporator and super-heater), internal recuperator and LNG condenser were modelled in part-load by correcting the UA values with a relationship proposed by Incropera [51]:

$$UA = UA_{des} \left(\frac{\dot{m}}{\dot{m}_{des}} \right)^{n}, \tag{2}$$

Equation (2) was derived assuming that the overall heat transfer coefficient is governed primarily by the heat transfer on one of the heat exchanger's sides. Therefore, it can directly be applied to the exhaust gas boiler and the LNG condenser, where the thermal resistance of the gas side (exhaust or LNG) is the dominating factor for the overall heat transfer coefficient. Manente et al. [45] employed a similar procedure for the estimation of the part-load performance of an ORC unit harvesting heat from a geothermal brine and selected the ORC fluid as the dominating heat transfer fluid. Consistently, the ORC fluid was selected herein as the limiting heat transfer fluid in the jacket cooling water preheater and superheater. This work considered shell and tube heat exchangers and the exponent n in Eq. (3) was set to 0.80 or 0.60 depending on the fluid location (inside or outside the tube banks). It was assumed that the LNG preheater is a multi-pipe heat exchanger due to the high operating pressure. Table 4 shows the selected dominating heat transfer fluid and exponents n for the various heat exchangers.

Table 4. Considered mass flows and exponents n for the heat exchangers calculations

Heat exchanger	Limiting heat transfer fluid	n
Preheater/evaporator/superheater (case A)	Exhaust gases	0.60
Preheater/superheater (case B)	ORC fluid	0.80
Evaporator (case B)	Jacket cooling water	0.60
LNG condenser	LNG	0.80
Recuperator	ORC fluid	0.60

The seawater condenser was modeled as a constant pressure heat exchanger in all the cases. The part-load calculations were limited to the working fluid with the best design-point performance. The following control criteria were considered for the off-design operation of the ORC configurations:

- For configurations A1 and A2, the boiler feed temperature and the fluid superheating at the inlet of the turbine were kept constant by controlling the rotational speed of pump 1. A throttling valve between the exhaust gas boiler and the turbine was activated in case the pressure at the turbine inlet dropped below a value corresponding to the saturation pressure at 115 °C. This prevented the fluid to enter the exhaust gas boiler in two-phase condition.
- In configurations A2 and B2, the LNG condenser pressure was kept constant by controlling the rotational speed of pump 2 and by activating a throttling valve between the two turbines.
- For configuration A3, pump 1 was considered as one component with variable rotational speed. The rotational speed was controlled in order to maintain a constant exhaust gas boiler feed temperature. In this case, the throttling valve was used to enforce a 20 % linear decrease of the boiler pressure from the design point value at 75 % main engine load the lowest load point corresponding to 25 % main engine load. This ensured efficient part-load operation.
- The temperature of the jacket water at the outlet of the heat recovery boiler was kept constant in configurations B1, B2 and B3.

- For configurations B1 and B2, the fluid superheating at the inlet of the turbine was kept constant by controlling the rotational speed of pump 1. Throttling valves were activated in case the superheating dropped below the design value.
- In configuration B3, the rotational speed of pump 1 was controlled in order to maintain a constant temperature at the inlet of the turbine, as this resulted in higher part-load performances compared to operation with a constant superheating degree.

The annual fuel saving potential of every configuration was assessed considering that the engine operates according to a typical load profile of a containership, see Fig. 2. The study was limited to the LNG fuel consumption: the pilot oil consumption, accounting for 4 – 10 % the fuel input, was neglected. Two scenarios were investigated for the use of the ORC power. In the first case, it was assumed that the ORC power could be directly utilized for propulsion, enabling the operation of the main engine at reduced loads. The electrical generator efficiency was here set to unity, as the ORC power output was utilized as mechanical power. The fuel savings were calculated as follows:

$$Fuel\ saving\ (\%) = 1 - \frac{Main\ engine\ annual\ consumption\ (with\ ORC)}{Main\ engine\ annual\ consumption\ (without\ ORC)}, \quad (3)$$

The behavior of the main engine and of the ORC unit below 25 % load were derived by extrapolating the obtained off-design performance curves. The ORC maximum power production was fixed to its design value, in order to avoid issues related to the mechanical and thermal limitations of its components. The extrapolation of the engine operational data below 25 % was considered acceptable since the engine load, even considering the contribution of the power provided by the ORC unit, was never below 23 %. In the second scenario, it was assumed that the power produced by the ORC was utilized to partly replace the electricity production of the onboard auxiliary engines. It was assumed that the energy demand on board the vessel was always higher or equal to the ORC power production and that the average consumption of the auxiliary engines was 160 g/kWh [52]. The incidence of the presence of the pilot oil on the fuel consumptions was assumed to be negligible and thus the savings were estimated by considering that the generators were supplied by pure LNG. The equivalent fuel saving, representing the ratio between the LNG saved in the auxiliary engines and the total consumption in the main engine, was calculated as:

$$Equivalent\ \ fuel\ saving\ (\%) = \frac{Annual\ saving\ in\ auxiliary\ engines}{Main\ engine\ annual\ consumption\ (without\ ORC)}, \quad (4)$$

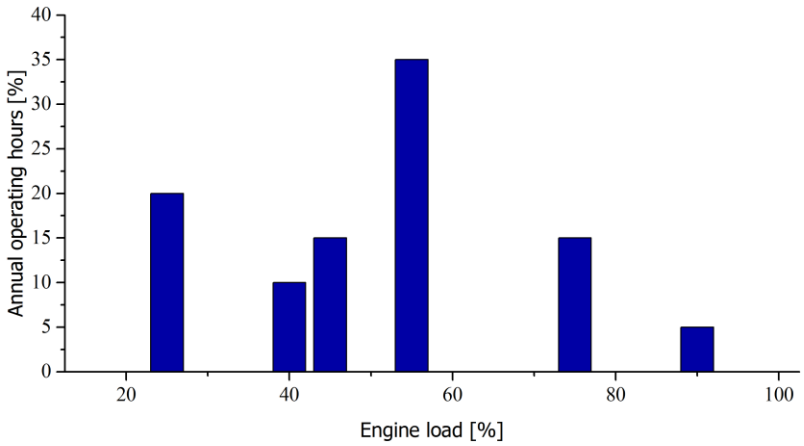

Fig. 2. Typical main engine load profile of a containership

3. Results and discussion

Tables 5 shows the results of the design case optimization for the configurations of case A. Table 6 shows the results for the configurations of case B. Figures 3 and 4 show a comparison of the net power output obtained with the various configurations. The use of an ORC unit exploiting the main engine exhaust gases and jacket cooling water (configuration A1) resulted in a net power output in the range 1,478 – 1,679 kW with a thermal efficiency from 16.3 % to 18.3 %.

Table 5. Optimization results for the ORC configurations case A

Fluid	$\dot{W}_{net}$ [kW]	η_{th} [-]	P_{boil} [bar]	TIT [°C]	$\dot{m}_{t1}$ [kg/s]	$P_{cond,1}$ [bar]	$P_{cond,2}$ [bar]	$T_{LNG,cond}$ [°C]	$\dot{m}_{t2}$ [kg/s]
Configuration A1									
R245fa	1679.58	16.66	29.21	206.89	33.35	1.78	-	-	-
MM	1651.45	16.90	5.51	177.90	24.63	0.07	-	-	-
butane	1641.33	16.26	30.00	200.33	17.50	2.83	-	-	-
ipentane	1630.04	18.35	27.00	206.27	15.64	1.09	-	-	-
n-Pentane	1566.94	18.23	20.35	203.18	14.49	0.82	-	-	-
isobutane	1513.89	14.50	29.03	191.15	19.89	4.05	-	-	-
cyclopentane	1504.33	18.02	9.59	205.05	13.76	0.51	-	-	-
Toluene	1478.36	17.7	1.83	204.70	13.82	0.05	-	-	-
Configuration A2									
R245fa	1781.42	17.54	29.21	209.28	32.76	1.78	0.051	-41.57	1.69
butane	1753.04	17.22	29.91	202.09	17.24	2.83	0.060	-57.37	0.76
ipentane	1716.95	19.11	25.52	206.40	15.42	1.09	0.045	-39.27	1.00
n-Pentane	1664.08	18.56	17.67	200.94	14.81	0.82	0.046	-31.69	1.03
isobutane	1631.95	15.53	29.03	193.70	19.56	4.05	0.060	-66.73	0.72
cyclopentane	1592.23	18.64	9.04	206.49	13.83	0.51	0.046	-21.39	1.04
Configuration A3									
n-Pentane	243.35	32.55	26.96	233.00	1.39	-	0.250	0.56	-
ipentane	243.29	34.20	27.01	233.00	1.35	-	0.237	-8.41	-
cyclopentane	227.45	29.34	14.16	233.00	1.38	-	0.247	12.02	-
butane	224.36	33.78	29.29	233.00	1.22	-	0.612	-13.08	-
isobutane	219.07	35.64	29.03	233.00	1.20	-	0.652	-22.50	-
R245fa	217.21	31.57	29.21	233.00	2.55	-	0.486	-1.85	-

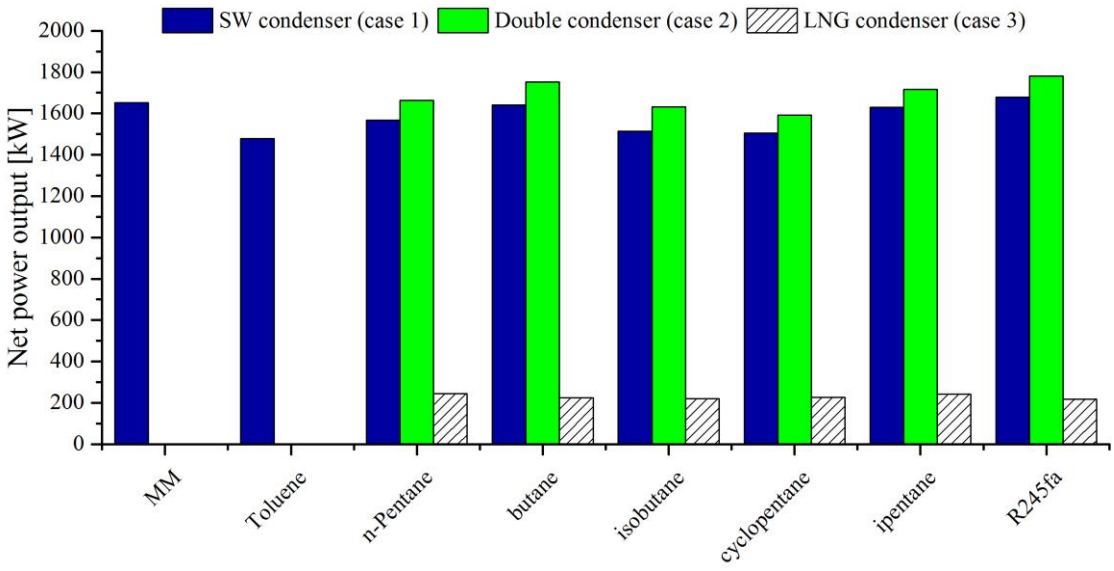

Fig. 3. Net power output in the various ORC configurations of case A

Table 6. Optimization results for the ORC configurations case B

Fluid	$\dot{W}_{net}$ [kW]	η_{th} [-]	P_{boil} [bar]	TIT [°C]	$\dot{m}_{t1}$ [kg/s]	$P_{cond,1}$ [bar]	$P_{cond,2}$ [bar]	$T_{LNG,cond}$ [°C]	$\dot{m}_{t2}$ [kg/s]
Configuration B1									
cyclopentane	241.58	7.62	1.97	79.44	6.83	0.51	-	-	-
R1233zd(E)	232.56	7.34	5.35	76.80	14.30	1.55	-	-	-
n-Pentane	231.66	7.31	2.96	76.66	7.24	0.82	-	-	-
R245fa	229.83	7.25	6.42	77.06	14.24	1.78	-	-	-
ipentane	229.71	7.25	3.73	76.77	7.62	1.09	-	-	-
butane	228.90	7.22	8.45	76.91	7.47	2.83	-	-	-
isobutane	224.53	7.08	11.41	77.20	8.20	4.05	-	-	-
R134a	220.02	6.94	22.51	80.00	16.12	7.70	-	-	-
Configuration B2									
butane	314.15	9.91	8.52	79.77	7.02	2.83	0.052	-59.48	0.74
ipentane	311.99	9.84	3.77	77.26	7.25	1.09	0.045	-39.23	1.00
R1233zd(E)	310.99	9.81	5.40	79.28	13.50	1.55	0.046	-42.89	1.66
cyclopentane	310.24	9.79	1.98	79.46	6.63	0.51	0.045	-21.60	1.03
R245fa	309.38	9.76	6.48	79.98	13.36	1.78	0.045	-43.43	1.65
isobutane	309.19	9.75	11.50	79.52	7.70	4.05	0.08	-62.56	0.76
n-Pentane	308.66	9.74	2.99	77.06	6.91	0.82	0.047	-31.33	1.02
R134a	291.49	9.20	22.71	80.00	15.34	7.70	0.369	-46.05	1.59
R1234yf	288.27	9.09	22.18	80.00	17.85	7.84	0.368	-50.30	1.85
Configuration B3									
ipentane	122.89	21.60	4.05	80.00	1.00	-	0.045	-39.25	-
n-Pentane	120.96	20.39	3.24	80.00	1.02	-	0.045	-31.96	-
butane	118.18	22.95	9.06	80.00	0.85	-	0.109	-47.56	-
isobutane	116.44	22.59	12.08	80.00	0.91	-	0.192	-47.63	-
R245fa	115.69	21.86	6.95	80.00	1.67	-	0.049	-42.41	-
R1233zd(E)	115.01	21.82	5.81	80.00	1.69	-	0.050	-41.44	-
cyclopentane	112.22	19.61	2.20	80.00	1.04	-	0.045	-21.62	-

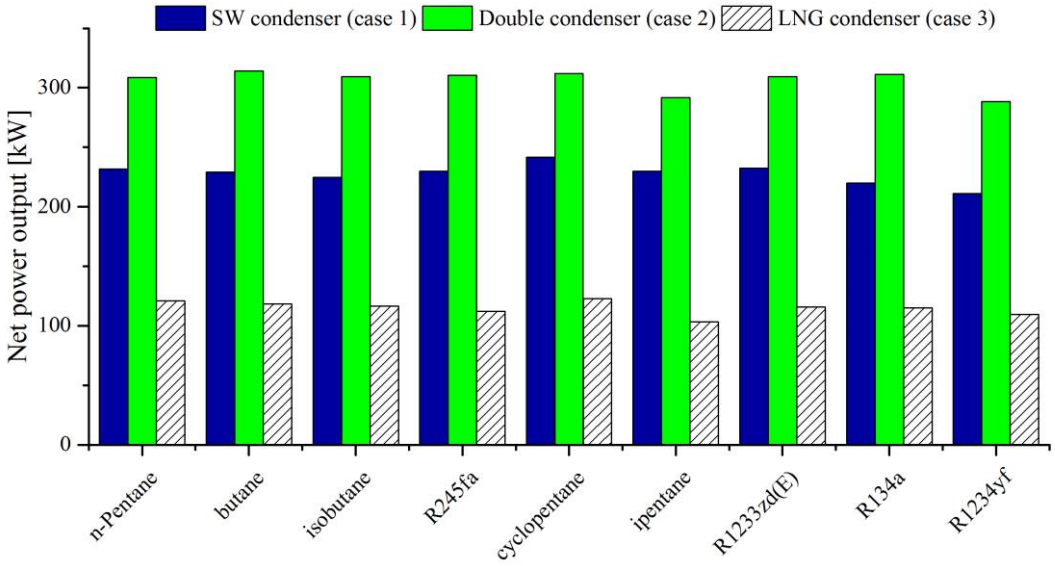

Fig. 4. Net power output in the various ORC configurations of case B

When the cycle featured an additional turbine, using also the cold energy of the LNG preheating process (configuration A2), the net power output increased up to 1781 kW. The implementation of the second turbine resulted in a net power output increment of around 6 %. Due to the constraint in

the minimum ORC pressure, MM and toluene were not considered for configurations A2 and A3. The exploitation of the jacket cooling water only (configuration B1) resulted in ORC units producing a net power output in the range 210 – 243 kW, while the implementation of the second turbine (configuration B2) resulted in an increase of the net power output up to 314 kW. In this case, the increase of power production was between 26.9 % and 41.3 %. The implementation of configurations using only the LNG pre-heating in the condenser (A3 and B3) resulted in lower power productions in comparison to the other cases, but enabled the attainment of high thermal efficiencies. If the cycle utilized both the engine exhaust gases and jacket water cooling (configuration A3), the thermal efficiency could be as high as 35.6 %, while an efficiency of 22.9 % could be obtained utilizing the jacket water and the LNG pre-heating (configuration B3). The lower power production of the configurations A3 and B3 is related to limited amount of fuel mass flow, which sets a constraint on the ORC mass flow rate. Figures 5 and 6 depict the results of the part-load investigations for the configurations of case A and B, respectively.

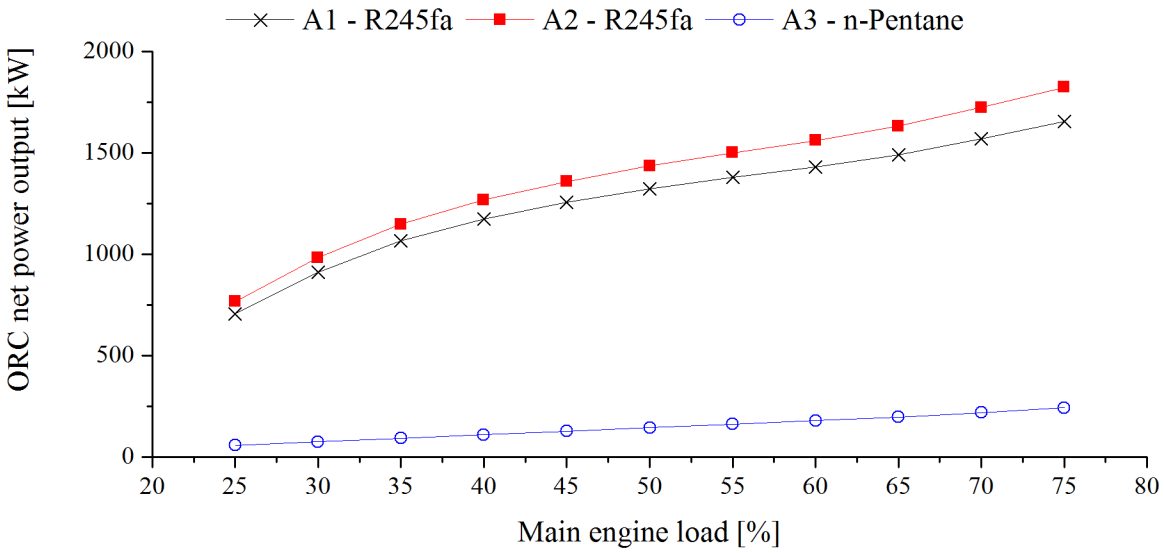

Fig. 5. Part-load performance of the ORC configurations case A

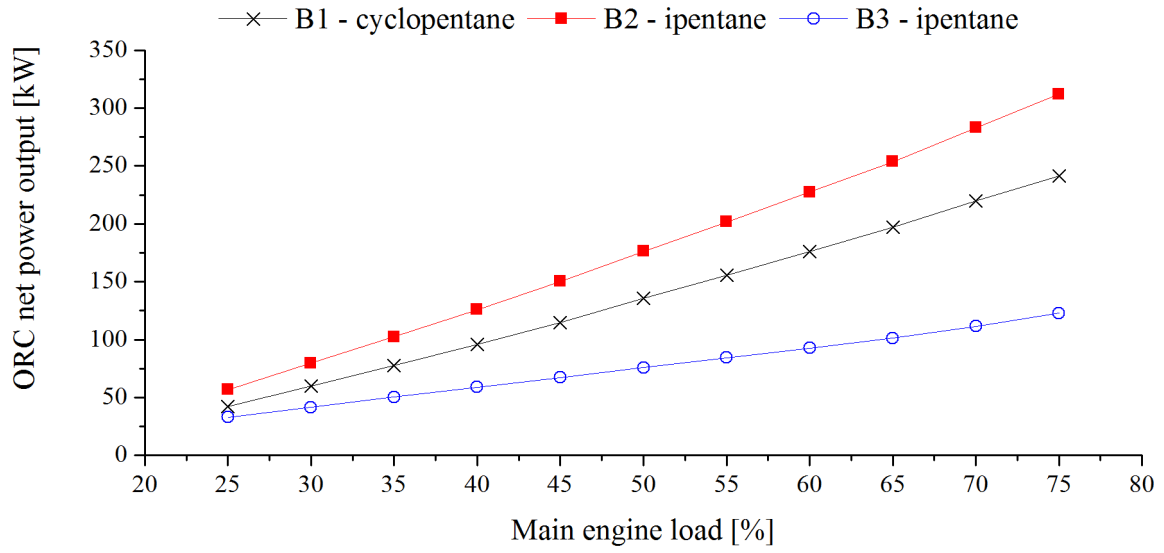

Fig. 6. Part-load performance of the ORC configurations case B

The results indicated that the ORC behavior was highly influenced by the considered heat sources. The ORC power output decreased almost linearly when the selected heat source was the jacket cooling water. Conversely, it had a non-linear trend when the heat source included also the exhaust

gases. Moreover, the net power output of the ORC configurations utilizing only the jacket water decreased much more sharply, reaching around 17 % of the design power output when the engine load was 25 %. On the contrary, when the main engine operated at 25 % load, the net power output was still above 40 % of the design value for case A configurations. This is strictly related to the way the various waste heat sources vary: the JW temperature is constant throughout the engine load, while the exhaust gases temperature increases as the engine operates at lower regimes (see Table 1), enabling to keep the ORC power production high. Comparing the solutions that feature only the seawater condenser with those utilizing a double condenser configuration, it appeared that the inclusion of the additional equipment resulted in an increment of the cycle power production over the whole load range of the main engine. However, the net power output difference between the two configurations decreases with the load. This is related to the fact that the fraction of mass flow rate supplied to the additional turbine depended on the amount of LNG required by the main engine, which decreased when the engine operated at low loads.

Table 7 shows the results of the annual simulations for the various configurations. The highest savings could be obtained by implementing configurations A1 or A2. When the ORC power production was directly utilized for propulsion, the fuel saving was 6.9 % for configuration A1 and 7.3 % for configuration A2. When the ORC production was utilized to replace the auxiliary engines, the fuel saving increased to 8.5 % and 8.9 %, for configurations A1 and A2 respectively. This difference is mainly due to two reasons. First, the power production from the ORC is higher when its energy output is utilized for electrical generation, because the load of the main engine is not reduced. Second, the thermal efficiency of the auxiliary engines is generally lower than the efficiency of the main engine. The estimated fuel saving for these cases (configurations A1 and A2) was between 1,075 and 1,391 ton/year. The estimated fuel saving for the configurations utilizing the main engine exhaust gases is aligned with previous studies in literature for HFO-fuelled ships: Larsen et al. [16] estimated a fuel saving of 5 %, while Baldi et al. [45] estimated a fuel saving potential of 7 % when neglecting the auxiliary heat needs on board.

The cases A1 and A2 were also simulated with a constraint on the minimum feed boiler temperature of 120 °C and 130 °C. The additional simulations showed a strong correlation between the minimum feed boiler temperature and the obtainable savings. For these cases, the equivalent fuel savings dropped by 3.2 – 5.9 % and 9.1 – 10.6 % respectively. The configurations utilizing only the jacket cooling water as heat source (case B) enabled lower fuel savings, up to 1 % for the first scenario and to 1.2 % for the second scenario. The annual fuel savings were estimated in the range 124 - 186 ton for cases B1 and B2, depending on the selected configuration and on the use of ORC power production.

Table 7. Results of the annual simulation for the two selected scenarios

	Use for propulsion			Use for auxiliary engines		
Configuration	ORC production [MWh]	Fuel saving [ton]	Fuel saving [%]	ORC production [MWh]	Fuel saving [ton]	Equivalent Fuel saving [%]
A1	8,048	1,075	6.9	8,283	1,325	8.5
A2	8,497	1,136	7.3	8,691	1,391	8.9
A3	981	131	0.8	960	154	1.0
B1	923	124	0.8	898	144	0.9
B2	1,191	160	1.0	1,163	186	1.2
B3	511	68	0.4	498	80	0.5

4. Conclusions

This study investigated the fuel saving potential of six different ORC configurations on board LNG-fuelled ships. The selected heat sources were the exhaust gases and the engine jacket cooling water, while the seawater and the cold energy released by the LNG during its preheating were considered as possible heat sinks. In addition, a novel ORC configuration that rejects heat to two heat sinks was described and discussed. The design of ORC configurations was optimized in order to maximize the net power output when the main engine operates at 75 % load and, subsequently, part-load performance curves were obtained. Two scenarios were proposed for the use of electrical power generated by the ORC unit. In the first one, the power was directly utilized for propulsion and thus fuel savings were achieved due to the reduction of the main engine load. In the second scenario, the ORC power output was utilized to fulfil the electricity demand on board, leading to a decrement of the fuel consumption of the auxiliary generators.

The results of the ORC unit design optimization showed that the highest net power outputs could be obtained when the unit harvests heat from both the exhaust gases and the jacket cooling water. In this case, the ORC unit produced a net power output of 1,478 – 1,679 kW with a thermal efficiency between 16.3 % and 18.3 %. By adopting a second turbine, which allowed the exploitation of the cold energy of LNG preheating, the power production increased up to 1,781 kW. The exploitation of the jacket cooling water heat resulted in lower net power outputs, in the range 210 – 243 kW, which could be increased up to 314 kW by adding the second ORC turbine. At part-load operation, the configurations utilizing both the exhaust gases and the jacket cooling water showed the highest performance. When the engine operates at 25 % load, the net power output of the ORC units utilizing both heat sources was around 40 % of the design value, while the net power output decreased to 17 % of its design value when utilizing only the jacket cooling water. The estimated fuel savings were between 6.9 % and 8.9 % using both heat sources and decreased to 0.8 – 1.2 % using only the jacket cooling water. The highest savings were attained using the ORC net power output for on board electricity supply, due to the low efficiency of the onboard generators and to the higher power production in the ORC unit.

Additional fuel savings are expected by optimizing the ORC unit including part-load considerations and by simultaneously optimizing the ORC unit and the main engine tuning [47, 53]. Future work includes more detailed analysis regarding the minimum allowable boiler feed temperature and the optimization of the cycle performance by taking into account the turbine design and performance.

Nomenclature

Abbreviations

Ex	exhaust gases
in	inlet
JW	jacket water
LNG	liquefied natural gas
ORC	organic Rankine cycle
out	outlet
TIT	turbine inlet temperature

Symbols

$\dot{m}$	mass flow rate, kg/s
P	pressure, bar
T	Temperature, °C

UA overall heat transfer coefficient, kWm^2/K

$\dot{W}$ power, kW

Greek symbols

η efficiency

Δ difference

Subscripts

boil boiler

cond condenser

des design

gear gearbox

gen generator

is isentropic

p pump

pp pinch point

rec recuperator

sw seawater

t turbine

References

[1] Burel F., Taccani, R., Zuliani, N., Improving sustainability of maritime transport through utilization of Liquefied Natural Gas (LNG) for propulsion. Energy 2013;57:412–420.

[2] IMO, Resolution MEPC.203(62), Amendments to the annex of the protocol of 1997 to amend the international convention for the prevention of pollution from ships, 1973, as modified by the protocol of 1978 relating thereto (Inclusion of regulations on energy efficiency for ships in MARPOL Annex VI), MEPC 62/24/Add. 1, London: International Maritime Organization; 2011.

[3] IMO, Resolution MEPC.212(63), Guidelines on the method of calculation of the attained energy efficiency index (EEDI) for new ships. MEPC 63/23, London: International Maritime Organization; 2012a.

[4] IMO, Resolution MEPC.213(63), Guidelines for the development of a ship efficiency management plan (SEEMP), MEPC 63/23, London: International Maritime Organization; 2012b.

[5] IMO, Sulfur oxides (SO_x) – Regulation 14. London: International Maritime Organization.

[6] IMO, Nitrogen Oxides (NO_x) – Regulation 13. London: International Maritime Organization.

[7] Levander O., New concepts in Ferries propulsion. Wärtsila Publication 2009:1-11.

[8] MAN Diesel and Turbo, Exhaust gas emission control today and tomorrow – application on MAN B&W two-stroke marine diesel engines. Publication No. 5510-0060-00, Copenhagen, Denmark, 2008.

[9] Wärtsilä, Wärtsila environmental product guide, Issue 2/2013, Wärtsila Finland Oy, 2013.

[10] Curt B., Marine transportation of LNG. Presentation at the Intertanko conference, March 29, 2004.

[11] Nordtun T., Sailing on LNG from concept to reality. Gas fuelled ships conference, Bergen, Norway, 12-14 September 2012.

[12] Smith A.B., Gas fuelled ships: fundamentals, benefits classification & operational issues. Proceedings of the first gas fuelled conference, Hamburg, Germany, 2010.

[13] The Mærsk group, http://www.maersk.com/en/hardware/triple-e/environment, [accessed: 22/11/2016].

[14] H. Öhman, P. Lundqvist, Comparison and analysis of performance using low temperature power cycles. Applied Thermal Engineering 2013; 52 (1):160–169.
[15] DTU Mechanical Engineering, PilotORC project, http://www.pilotorc.mek.dtu.dk, [accessed: 22/11/2016].
[16] Larsen U., Sigthorsson O., Haglind F., A comparison of advanced heat recovery power cycles in a combined cycle for large ships. Energy 2014;74:260-268.
[17] Andreasen J. G., Meroni A., Haglind F., A comparison of organic and steam Rankine cycle waste heat recovery systems on ships. Energies 2017; 10(4), 547.
[18] MAN Diesel and Turbo, Soot deposits and Fires in Exhaust gas Boilers. http://marine.man.eu/docs/librariesprovider6/technical-papers/soot-deposits-and-fires-in-exhaust-gas-boilers.pdf?sfvrsn=23 [accessed: 22/11/2016].
[19] Kumar S., Kwon H-T., Choi K-H., Lim W., Cho J. H., Tak K., Moon I., LNG: An eco-friendly cryogenic fuel for sustainable development. Applied Energy 2011; 88:4264–4273.
[20] Romero Gómez M., Ferreiro Garcia R., Romero Gómez R., Carbia Carril J., Review of thermal cycles exploiting the exergy of liquefied natural gas in the regasification process. Renewable and Sustainable Energy Reviews 2014; 38:781 - 795.
[21] Sung T., Kim K. C., Thermodynamic analysis of a novel dual-loop organic Rankine cycle for engine waste heat and LNG cold. Applied Thermal Engineering 2016;100:1031–1041.
[22] Soffiato M., Frangopoulos C., Manente G., Rech S., Lazzaretto A., Design optimization of orc system for waste heat recovery on board a LNG carrier. Energy Conversion and Management 2015;92:523-534.
[23] Senary K., Tawfik A., Hegazy E., Ali A., Development of a waste heat recovery system onboard LNG carrier to meet IMO regulations. Alexandria Engineering Journal 2016;55:1951-1960.
[24] MAN Diesel & Turbo, CEAS calculation tool, http://marine.man.eu/two-stroke/ceas [Accessed: 23.11.2016].
[25] MAN Diesel & Turbo, ME-GI Gas-ready Ship. http://marine.man.eu/docs/librariesprovider6/test/me-gi-gas-ready-ship-low.pdf?sfvrsn=6 [Accessed: 23.11.2016].
[26] Larsen U., Pierobon L., Haglind F., Gabrielii C., Design and optimization of organic Rankine cycles for waste heat recovery in marine applications using the principles of natural selection. Energy 2013;55:803–812.
[27] Bao J., Zhao L., A review of working fluid and expander selections for organic Rankine cycle. Renewable and Sustainable Energy Reviews 2013;24:325–342.
[28] Song J., Song Y., Gu W., Thermodynamic analysis and performance optimization of an Organic Rankine Cycle (ORC) waste heat recovery system for marine diesel engines. Energy 2015;82:976-985.
[29] Wang D., Ling X., Peng H., Liu L., Tao L., Efficiency and optimal performance evaluation of organic Rankine cycle for low grade waste heat power generation. Energy 2013;50(1):343-352.
[30] Yang M-H, Yeh R-H, Analyzing the optimization of an organic Rankine cycle system for recovering waste heat from a large marine engine containing a cooling water system. Energy Conversion and Management 2014;88:999-1010.
[31] Kim K., Lee U., Kim C., Han C., Design and optimization of cascade organic Rankine cycle for recoverying cryogenic energy from liquefied natural gas using binary working fluids. Energy 2015;88:304-313.
[32] He S., Chang H., Zhang X., Shu S., Duan C., Working fluid selection for an Organic Rankine Cycle utilizing high and low temperature energy of an LNG engine. Applied Thermal Engineering 2015;90:1579-1589.
[33] Quoilin S., Van Den Broek M., Declaye S., Dewallef P., Lemort V., Techno-economic survey of Organic Rankine Cycle (ORC) systems. Renewable and Sustainable Energy Reviews 2013; 22:168–186.

[34] Colonna P., Casati E., Trapp C., Mathijssen T., Larjola J., Turunen-Saaresti T., Uusitalo A., Organic Rankine Cycle Power Systems: From the Concept to Current Technology, Applications, and an Outlook to the Future. Journal of Engineering for Gas Turbines and Power 2015; 37(10):1-19.
[35] Ömann H., Lundqvist P., Screw expanders in ORC applications, review and a new perspective. 3rd International Seminar on ORC Power Systems, October 12-14, Brussels, Belgium, 2015:1-10.
[36] Invernizzi C. M., Bonalumi D., Thermal stability of organic fluids for Organic Rankine Cycle systems. In: Macchi E., Astolfi F., editors. Organic Rankine Cycle (ORC) Power systems. Woodhead Publishing, 1st edition. 2016. p. 121-151.
[37] Zyhowski G, Brown A., Low global warming fluids for replacement of HFC-245fa and HFC-134a in ORC applications. Proceedings of ECOS 2011: the 24th international conference on Efficiency, Cost, Optimization, Simulation and Environmental Impact of Energy Systems, Novi Sad, Serbia, 2011.
[38] Bell I. H., Wronski J., Quoilin S., Lemort V., Pure and Pseudo-pure Fluid Thermophysical Property Evaluation and the Open-source Thermophysical Property Library CoolProp. Industry & Engineering Chemistry Research 2014;53(6):2498-2508.
[39] Rayegan R., Tao Y., A procedure to select working fluids for Solar Organic Rankine Cycles (ORCs). Renewable Energy 2011;36(2):659-670.
[40] Drescher U., Brüggermann D., Fluid selection for the Organic Rankine cycle (ORC) in biomass power and heat plants. Applied Thermal Engineering 2007;27(1):223-228.
[41] Man Diesel & Turbo, Waste Heat Recovery System (WHRS) – Marine Engines & Systems. http://marine.man.eu/docs/librariesprovider6/technical-papers/waste-heat-recovery-system.pdf?sfvrsn=10 [Accessed: 23.11.2016].
[42] Andreasen J.G., Larsen U., Knudsen T., Pierobon L., Haglind F., Selection and optimization of pure and mixed working fluids for low grade heat utilization using organic Rankine cycles. Energy 2014;73:204 -213.
[43] Schobeiri, M., Turbomachinery flow physics and dynamic performance. Berlin, Germany: Springer Berlin; 2005.
[44] Stodola A., Dampf-und Gasturbinen: Mit einem Anhang über dei Aussichten der Wärmekraftmaschinene. Berlin, Germany, Springer Berlin: 1922.
[45] Manente G., Toffolo A., Lazzaretto A., Paci M., An Organic Rankine Cycle off-design model for the search of the optimal control strategy. Energy 2013;58:97-106.
[46] Wang J., Yan Z., Zhao P., Dai Y., Off-design performance analysis of a solar-powered organic Rankine cycle. Energy Conversion and Management 2014;80:150-157.
[47] Baldi F., Larsen U., Gabrielii C., Comparison of different procedures for the optimization of a combined Diesel Engine and organic Rankine cycle system based on ship operational profile. Ocean Engineering 2015;110:85–93.
[48] Pierobon L., Benato A., Scolari E., Haglind F., Stoppato A., Waste heat recovery technologies for offshore platforms. Applied Energy 2014;163:228-241.
[49] Haglind F., Elmegaard B., Methodologies for predicting the part-load performance of aero-derivate gas turbines. Energy 2009;34(10):1484-1492.
[50] CR – Innovation inside, Technical brochure from Grundfos official website. http://www.grundfos.com/products/find-product/CR-CRE-CRN-CRNE-CRI-CRIE-CRT-CRTE.html#brochures. [accessed 24.02.2015].
[51] Incropera F. P., DeWitt D. P., Bergman T. L., Lavine A. S., Fundamentals of Heat and Mass transfer. 6th Edition, John Wiley & Sons, Inc: Jefferson City, MO, USA, 2007.
[52] Kristensen H. O., Energy demand and exhaust gas emissions of marine engines. Clean Shipping Currents 2012:6.
[53] Larsen U., Pierobon L., Baldi F., Haglind F., Ivarsson A., Development of a model for the prediction of the fuel consumption and nitrogen oxides emissions trade-off for large ships. Energy 2015;80:545-555.